Modified polymer matrix in pharmaceutical hot melt extrusion by molecular interactions with a carboxylic co-former

Felix Ditzinger[1,2], Uta Scherer[3], Monica Schönenberger[4], René Holm[5,6], Martin Kuentz[2]

[1] University of Basel, Department of Pharmaceutical Sciences, Basel, Switzerland

[2] University of Applied Sciences and Arts Northwestern Switzerland, Institute of Pharma Technology, Muttenz, Switzerland

[3] University of Applied Sciences and Arts Northwestern Switzerland, Institute of Chemistry and Bioanalytics, Muttenz, Switzerland

[4] University of Basel, Swiss Nanoscience Institute (SNI) - Nano Imaging, Basel, Switzerland

[5] Drug Product Development, Janssen Research and Development, Johnson and Johnson, Beerse, Belgium

[6] Department of Science and Environment, Roskilde University, 4000 Roskilde, Denmark

Corresponding author:

Prof. Dr. Martin Kuentz

University of Applied Sciences and Arts Northwestern Switzerland

Institute of Pharma Technology

Hofackerstr. 30

4132 Muttenz, Switzerland

Phone number: 0041 61 228 56 42

martin.kuentz@fhnw.ch

Abstract

Hot melt extrusion (HME) has become an essential technology to cope with an increasing number of poorly soluble drug candidates. However, there is only limited choice of pharmaceutical polymers to obtain suitable amorphous solid dispersions (ASD). Considerations of miscibility, stability, and biopharmaceutical performance narrow the selection of excipients and further technical constraints arise from the needed pharmaceutical processing. The present work introduces the concept of molecularly targeted interactions of a co-former with a polymer to design a new matrix for HME. Model systems of dimethylaminoethyl methacrylate copolymer, Eudragit E (EE) and bi-carboxylic acids were studied and pronounced molecular interactions were demonstrated by ^{1}H, ^{13}C NMR, FTIR spectroscopy as well as by different techniques of microscopic imaging. A difference was shown between new formulations exploiting specifically the targeted molecular interactions and a common drug-polymer formulation. More specifically, a modified matrix with malic acid exhibited a technical extrusion advantage over polymer alone and there was a benefit of improved physical stability revealed for the drug fenofibrate. This model compound displayed greatly enhanced dissolution kinetics from the ASD formulations. It can be concluded that harnessing molecularly designed polymer modifications by co-formers has much potential in solid dispersion technology and in particular regarding HME processing.

Keywords: Poorly water-soluble drug, enabling formulation, hot melt extrusion, co-former, polymeric modification, atomic force microscopy

1 Introduction

Poor water solubility of new drug candidates is a main pharmaceutical challenge to avoid erratic and highly variable absorption following oral administration. To facilitate effective and safe medications, bio-enabling formulations are needed and much research has centered around amorphous drug delivery systems.[1–4] There are a few methods available for drug amorphization, however, a recent overview of oral

drug products on the market based upon amorphous drug delivery systems, clearly demonstrated that spray drying and hot melt extrusion (HME) were the most abundant industrial manufacturing processes.[1,5] For physical stabilization of drugs in an amorphous form, there are some pharmaceutically accepted polymers available. However, specific process demands of spray drying or HME manufacturing define some limitations to this choice. This is also reflected by the use of few different polymers in the compositions of marketed solid dispersions.[5] Hence, new chemically engineered polymers would be desirable. However, the development and regulatory requirements [6] of a pharmaceutical excipient results in lengthy and costly processes. Another hurdle of chemical excipient modifications is the resulting permanent character. This permanent modification could lead to advantages regarding processing and physical stability, which may not always go along with the situation upon formulation hydration followed by a suitable drug release and supersaturation. Consequently, a non-permanent modification would be beneficial to overcome the previously mentioned difficulties.

Therefore, another approach to broaden the excipient landscape would be the combination of already approved polymers with interacting pharmaceutically acceptable small molecular compounds to obtain specifically designed matrices by co-processing. This could generate advantages with respect to dry formulation as well as improving the biopharmaceutical properties. This scope differs from classical addition of small molecular process aids that typically interact non-specifically without a clear molecular rationale.[7] Previous work on additives was either rather of an exploratory nature or it was, for example, intended to generate a pH microclimate upon release, which is a specific approach in its own right.[8] Different from the present study aims are also co-amorphous systems because the targeted interactions are directly between additive and active pharmaceutical ingredient (API).[9,10]

It was recently identified by Higashi [11] and co-workers that the creation of molecular interactions between a model drug and dimethylaminoethyl methacrylate copolymer, Eudragit E (EE) together with saccharine, as a small molecular additive, led to an improved drug dissolution behavior. The authors argued that saccharine was interacting via ionic or hydrogen bonding with the polymeric amino group. Drug interactions were in this case rather given by the hydrophobic side chains of the polymer. This was in line

with a recent study, which suggested that even basic drugs can exhibit great solubility enhancement with EE. [12,13] This may appear counter-intuitive given the same charges of drug and polymer at physiological pH. However, NMR data indicated that hydrophobic interactions of the drug with polymer were likely involved in the observed solubility increase. While the amino group can be beneficial for direct interactions with acidic drugs [13], it might be in other cases better masked or changed by specific additives.

Encouraged by finding of additive hydrophobic interaction of EE with lipophilic drugs, [12] a change of the amino group in EE could lead to a modified matrix that retains its ability to interact with hydrophobic compounds. A concern of this approach may be that masking of the hydrophilic amino group possibly decreases hydration and solubility of the modified polymer, hence an optimal interacting component may need to have an additional hydrophilic group to compensate.

Therefore, the aim is to use small-molecular additives to change specifically functional polymer groups. It is in this context possible to profit from analytical advancements and excipient screening in the science of co-amorphous formulations even though the latter field is quite different from that of modified matrices as the scope of co-amorphous complexes is to alter drug properties directly, for example regarding glass forming ability. [8,14]

In contrast to previous co-amorphous studies, [10,15,16] the idea to design a modified polymer matrix by small-molecular additives is a new approach and improvements regarding processing, stability, or biopharmaceutical performance can origin from such a co-processed system.[8] This work targets specific interactions of small molecular bi-valent acids with the amino group of EE. In line with the above-mentioned considerations, bi- valent acids mask the amino group of EE, while the second carboxy group is meant to retain sufficient polymer swelling and solubility. The hypothesis is whether such an approach is technically feasible and if it is possible to obtain clear benefits for amorphous solid dispersions of a poorly water-soluble model drug (i.e. fenofibrate).

2 Material and Methods

2.1 Materials

EE was kindly provided by Evonik industries (Essen, Germany), malic acid (MA) and the model drug fenofibrate (FE) were bought from Sigma-Aldrich (St. Louis, MO, USA). All compounds were used as received either in the initial co-processing of polymer and MA or for an alternative direct extrusion of all components by hot melt extrusion. The different compositions of the formulations as well as reference mixtures are outlined in Table 1. For a reference of the physical mixture, crystalline FE was used.

Table 1: Composition of the different extrudates and of physical mixture for comparison.

	Content MA [%]	Content EE [%]	Content FE [%]	Manufacturing[a]
Matrix	32.4	67.6	-	Extrusion, milling
Direct extrusion	27.5	57.5	15.0	Extrusion, milling
Matrix extrusion	27.5	57.5	15.0	Extrusion, milling, extrusion, milling
FE & EE extrusion	-	85.0	15.0	Extrusion, milling
Physical mixture	27.5	57.5	15.0	Milling

[a] The described processing steps were applied in the order mentioned.

2.2 Methods

2.2.1 Process of hot melt extrusion (HME)

The different solid dispersions were prepared by using the co-rotating twin-screw extruder ZE9 ECO from Three-Tec (Birren, Switzerland). A pair of screws with a diameter of 9 mm, a length of 180 mm was

used that consisted of conveying as well as mixing elements. Prior to extrusion, all ingredients were pre-mixed in a beaker to then manually fill the extruder with a spatula. The three heating zones of the extruder were set to 130 °C and a screw speed of 80 rpm was applied. After extrusion, the extrudates were cooled to room temperature and stored at ambient conditions in falcon tubes. The formulation called 'matrix extrusion' was manufactured by an initial extrusion of the polymer with additive (EE & MA) to obtain a co-processed matrix ('matrix extrusion') that was vibrational milled at 30/s for 1 min. A subsequent extrusion with addition of the model compound FE provided the final drug product. All other formulations (FE & EE & MA 'direct extrusion', and FE & EE) were manufactured in the process described by a single extrusion step. The physical mixture was obtained by mixing and consecutive milling (Table 1). All milled powders were sieved (mesh size 150 µm) to achieve a comparable particle size distribution.

2.2.2 Molecular interaction studies

2.2.2.1 Attenuated total reflectance Fourier-transform infrared spectroscopy (ATR-FTIR)

The FTIR spectra were measured by a Cary 680 Series FTIR spectrometer (Agilent Technologies, Santa Clara, USA) equipped with an attenuated total reflectance accessory. A scanning range of 4000–600 cm^{-1} was selected with 42 scans and a resolution of 4 cm^{-1}. The spectra were evaluated using the software ACD/Spectrus Processor 2016.1.1 (Advanced Chemistry Development Toronto, Canada).

2.2.2.2 Nuclear magnetic resonance spectroscopy (NMR)

The ^{13}C-NMR spectra were recorded at ambient conditions on a Bruker Avance III 400 NMR spectrometer (Bruker BioSpin AG, Fällanden, Switzerland) fitted with a 5 mm i.d. BBO prodigy probe and operating at 100.61 MHz. The number of scans was set to 1024. The samples were dissolved in deuterated DMSO and for processing the spectra, the software TopSpin 3.5pl7 from Bruker was used. Deuterated DMSO was selected because it would not interfere with the investigated interaction.[17] The solvent peak of DMSO served as reference for comparison of the spectra. Peaks were assigned using 2D heteronuclear single quantum coherence spectroscopy (HSQC) NMR measurements. Moreover, the

149 influence of molecular interactions between additive and polymer were also simulated by the software
150 ACD/C+H NMR Predictors 2016.1.1 (Advanced Chemistry Development Toronto, Canada) to support
151 interpretation of the NMR spectra.
152

153 **2.2.3 Stability assessment and drug dissolution**

154 **2.2.3.1 X-ray powder diffraction (XRPD)**

155 The analysis of an amorphous form by XRPD was performed on a D2 Phaser diffractometer (Bruker AXS
156 GmbH, Karlsruhe, Germany) with a 1-D Lynxeye detector. The instrument was equipped with a 1.8 kW
157 Co KFL tube providing x-ray radiation at a wavelength of 1.79 Å. During the measurements a voltage of
158 30 kV and a current of 10 mA were used. The increment and time per step were set to 0.02 ° and 2 s,
159 respectively. The measurements were performed over a range of 5 ° to 39 ° (2θ). To avoid the
160 recrystallization of the drug due over processing steps the extrudates were cut in 2 cm long pieces and
161 arranged to cover the complete sample holder of the instrument.
162

163 **2.2.3.2 Differential scanning calorimetry (DSC)**

164 Further solid state assessment of an amorphous form was based on thermal analysis by using a differential
165 scanning calorimeter DSC 3 (Mettler Toledo, Greifensee, Switzerland). The measurements were
166 conducted at a heating rate of 10 °C/min from -20 °C to 140 °C. The surrounding of the sample cell was
167 purged with nitrogen 200 mL/min. To evaluate the thermal history of the sample, the first heating was
168 used. The samples were cut into small pieces and 5 to 9 mg were placed in an aluminum pan with a
169 pierced lid. The thermal events were analyzed with the STARe Evaluation-Software Version 16 (Mettler
170 Toledo, Greifensee, Switzerland).
171

172 **2.2.3.3 Polarized light microscopy (PLM)**

173 An assessment of crystallinity was based on polarized light imaging using a microscope Olympus BX60
174 (Volketswil, Switzerland) equipped with a polarization filter. Extrudates that were transparent were
175 placed in the sample holder and analyzed by taking pictures with full polarized light to detect crystals as

birefringent spots. The images were compared with pictures in unpolarized light. All of these pictures were acquired with a digital camera XC30 from Olympus attached to the microscope. The magnification remained constant throughout the whole measurement (scale bars are displayed in every image).

2.2.3.4 Scanning electron microscopy (SEM) with energy dispersive X-ray spectroscopy (EDX)

Cross sections of the extrudates were analyzed with a SEM TM3030 Plus (Hitachi, Tokyo, Japan). Elemental constitution was evaluated using EDX with an acceleration voltage of 15 kV. The Quantax 70 system was employed, which consisted of an X Flash Min SVE signal processing unit, Megalink interface, a scan generator, and an X Flash silicon drift detector 410/30H (Bruker Nano GmbH, Berlin, Germany). Images were processed for detection of the halogen chloride to analyze the spatial distribution of FE on the sample.

2.2.3.5 Confocal laser scanning microscopy (CLSM)

The 3D CLSM (Keyence VK-X200) images were acquired on a Keyence VK-X200 confocal laser microscope with a wavelength of 408 nm to measure even larger areas of the samples. Image magnifications are shown in the pictures. Cross sections of the extrudates were evaluated after the cutting of the extrudates by a razor blade.

2.2.3.6 Atomic force microscopy (AFM)

Measurements were performed on a NanoWizard 4 from JPK (maximum XY scan range: 100 x 100 mm, Z-height maximum: 15 mm) at ambient conditions of 25 °C. The cantilever Tap190 was used in the so called tapping or AC (amplitude control) mode. In this mode the probe is oscillated near its mechanical resonance frequency. During each cycle of the oscillation the probe lightly taps the surface and the amplitude of oscillation is reduced due to damping or dissipation of energy already in close proximity of the interacting surface. The AFM system uses this change in amplitude to track the surface topography. If phase imaging mode is carried out, the phase shift relative to the driving oscillator is monitored in addition to the amplitude. Typically, the phase signal is sensitive to variations in composition, adhesion, friction, viscoelasticity as well as other factors. Therefore, material differences manifest in brighter and

darker regions in the phase images, comparable to the way topography changes are recorded in height images. The cantilever had a force constant of 48 N/m and a resonant frequency of 190 kHz. All pictures are given in a 512 x 512 pixels and adjusted coloring for comparison. Samples were cut to investigate the cross sections and placed into the sample holder of the instrument.

2.2.3.7 Dynamic flow properties

A rotating drum system (Revolution®, Mercury Scientific Inc., USA) was employed to measure powder flow properties. The powder movement in the barrel with a diameter of 55 mm and a width of 35 mm was scanned by a camera (resolution of 648 × 488 pixel). The acquired pictures at 10 frames per second were analyzed by the Revolution® V3.00 software (Mercury Scientific Inc., USA). Prior to the measurement, the drum was filled with a constant sample volume of 14.5 mL and the initial rotation time was set to 45 s. After that time 150 avalanches were monitored at a rotation speed of 1 rpm. All measurements were performed in triplicates. The measured properties were avalanche angle [°] and absolute break energy [mJ/kg].[18,19] The avalanche angle was recorded as the angle between the center point of the powder edge and the highest position before the occurrence of an avalanche. The absolute break energy was defined to be the maximum energy in the powder sample before the beginning of an avalanche. This value is considered as the required energy for the start of an avalanche. [18,19]

2.2.3.8 Comparison of dissolution behavior

Drug dissolution was studied for comparison of the extruded formulations and the physical mixture. Prior to dissolution, all samples including the physical mixture were milled in a vibrational mill for 1 min at a speed of 20/s. A USP II dissolution apparatus filled with phosphate buffer solution pH 6.4, as described by PhEur. 2.9.3, in combination with 0.5 % Sodium dodecyl sulfate was used. The paddle speed and temperature were set to 100 rpm and 37.0 °C, respectively. This experimental procedure was in accordance with quality control dissolution set-ups. [20] Upon withdrawal from the dissolution media, the samples were filtered through a 0.4 µm filter directly. Withdrawn medium was replaced immediately with temperature-controlled dissolution medium. Samples were analyzed by a high pressure liquid chromatography system from Agilent (Agilent Technologies, Santa Clara, United States of America)

equipped with an UV detector, which was set to 287 nm. The flowrate was set to 0.25 mL/min with a run time of 10 min and an injection volume of 20 µL. As separation reverse phase column a ZORBAX Elipse Plus C18 (Agilent Technologies, Santa Clara, United States of America) was used.

3 Results and discussion

3.1 Molecular considerations for polymer and co-former selection

The polymer selection is critical for any solid dispersion and should particularly consider the type of intended release as well as miscibility with a given drug. [21] It has been attempted previously to choose polymers based on *ab initio* considerations of molecular drug interactions[22], which should not only help to achieve a good kinetic stability of the solid dispersion, but also facilitate sustained supersaturation upon formulation dispersion. [23] Further selection criteria are linked to the intended processing (i.e. HME), why the glass transition temperature (T_g), the melting point (T_m), degradation temperature (T_{deg}) as well as the resulting melt viscosity at extrusion temperature should be considered. Optimal is of course when formulators could choose from a broad variety of alternative polymers to meet the technical needs of manufacturing, however such a selection is rather limited with pharmaceutically acceptable polymers. To generate more potential variations and thereby options, the current work hypothesized that co-processing of a polymer with small molecular additive could provide a specifically modified polymer matrix with advantages for solid dispersions produced by HME. The model polymer EE was selected for this purpose as the aminoalkyl group can interact with acidic small molecular additives in line with the scope of the current study. Moreover, the polymeric side chains of EE seem attractive regarding possible hydrophobic interactions with a drug. [12,13,24] Strong hydrogen bonding of a weak carboxylic acid with EE's tertiary amines have been reported and direct drug-polymer interactions were shown not to lead to any salt-formation. [25] Unlike this previous study, such polymer interactions were in the current work harnessed by bi-carboxylic additives. Those additives have proven to be beneficial for HME processing by Parikh and Serajuddin, although in their work the interaction was formed between an API and the acid. [26] Compared to monocarboxylic acids, the additional carboxy group should reduce the risk to make the EE polymer

matrix too hydrophobic upon aqueous dispersion in gastro-intestinal fluids. Thus, promising bi-carboxylic acid candidates included succinic acid, maleic acid, fumaric acid, tartaric acid, malonic acid, and MA, which were studied during initial extrusion trials with EE. For the assessment of amorphous stability, FE was chosen as a model drug due to its well-described amorphous instability. [27] Initial extrusion trials with different bi-carboxylic acids could not result in completely amorphous FE formulations as demonstrated by XRPD measurements or showed poor processing ability. Different mechanisms possibly contributed to less favorable extrusion results such as decomposition, differences in melt viscosity or melting point, or lack of miscibility. Based on the initial bi-carboxylic acid screening, a focus was made on the most promising compound, MA as co-former for EE.

3.2 Modified polymeric matrix

3.2.1 Molecular interaction

In line with the targeted molecular assembly of EE and MA, a first objective of this work was to verify the molecular interaction as well as the potential benefits for HME of EE and MA experimentally. Technical extrudability was indeed improved in presence of MA. Compared to pure EE, the ease of re-solidification and strand formation from the orifice of the extruder was improved in the modified matrix. The final product was a transparent and homogenous extrudate. FTIR measured on the extrudate (Figure 1) showed the broadening of the OH peak in the region of 3400 cm^{-1}, which led to a flatter, hardly detectable peak. This could be associated with MA, since it is the only molecule in the mixture with a free hydroxyl group. [16] It also has to be taken into account that the amorphous nature of the extrudate caused a rather general peak broadening. Moreover, a specifically broad peak holding for an asymmetrical stretching vibration at 1580 cm^{-1} was identified, which can be associated with hydrogen bonding interaction of the carboxylic group of MA.[28,29]

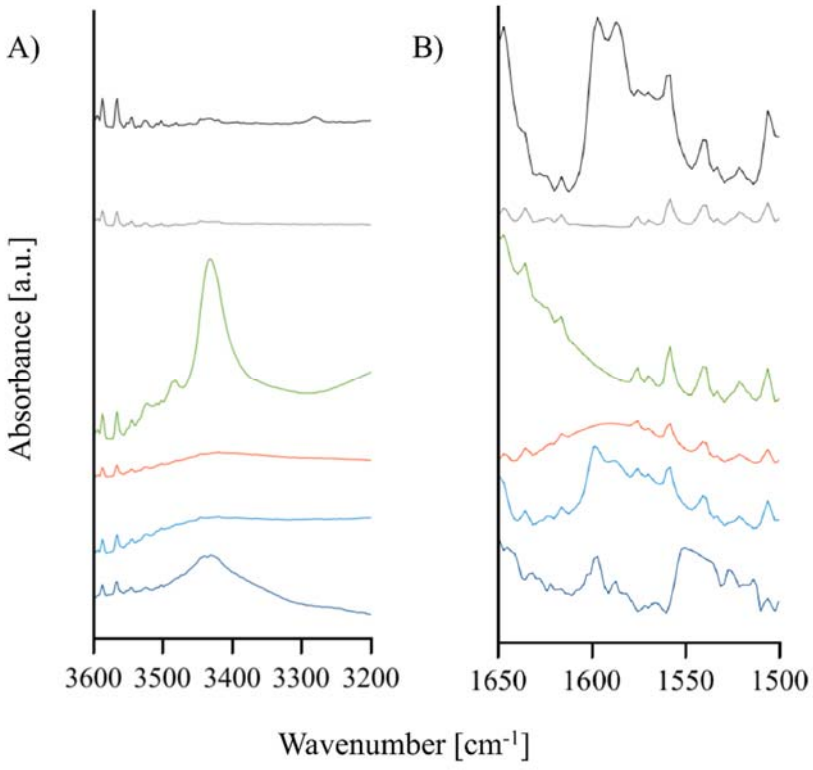

Figure 1: A) and B) show the FTIR spectra of the different formulations between 3200 – 3600 cm1 and 1500 – 1650 cm1, respectively. The curves represent powders of FE (black), EE (grey), MA (green), extrudates of MA & EE (red), FE & MA & EE (light blue), and the physical mixture of FE & MA & EE (dark blue).

The vibrational FTIR spectroscopy was complemented by NMR analysis. While in the ^{1}H-NMR, a differentiation between the different hydroxyl groups of MA and therefore their specific interaction with polymer was hardly detectable, ^{13}C-NMR was applied for a more detailed analysis. An interesting region for the two carboxylic groups of MA was shown between 172 and 176 ppm, which in the ^{13}C spectrum corresponds to a shift of the two carbons in the two carboxylic groups (Figure 2). In comparison to the pure MA, the spectrum of the extruded polymeric matrix showed a peak shift, which was more intense for the carboxylic group with an alpha hydroxyl group (Figure 2). Therefore, this group is likely to show an interaction with the polymer, which was formed during the extrusion. [24] Neither FE nor EE showed interfering peaks in the investigated region, because the ester peak of FE could be clearly distinguished from the carboxylic peaks of MA. The observed shift was in line with a simulation of the spectrum as calculated by the ACD/C+H NMR Predictor. Moreover, the same shift could be observed in the formulation with FE (Figure 2).

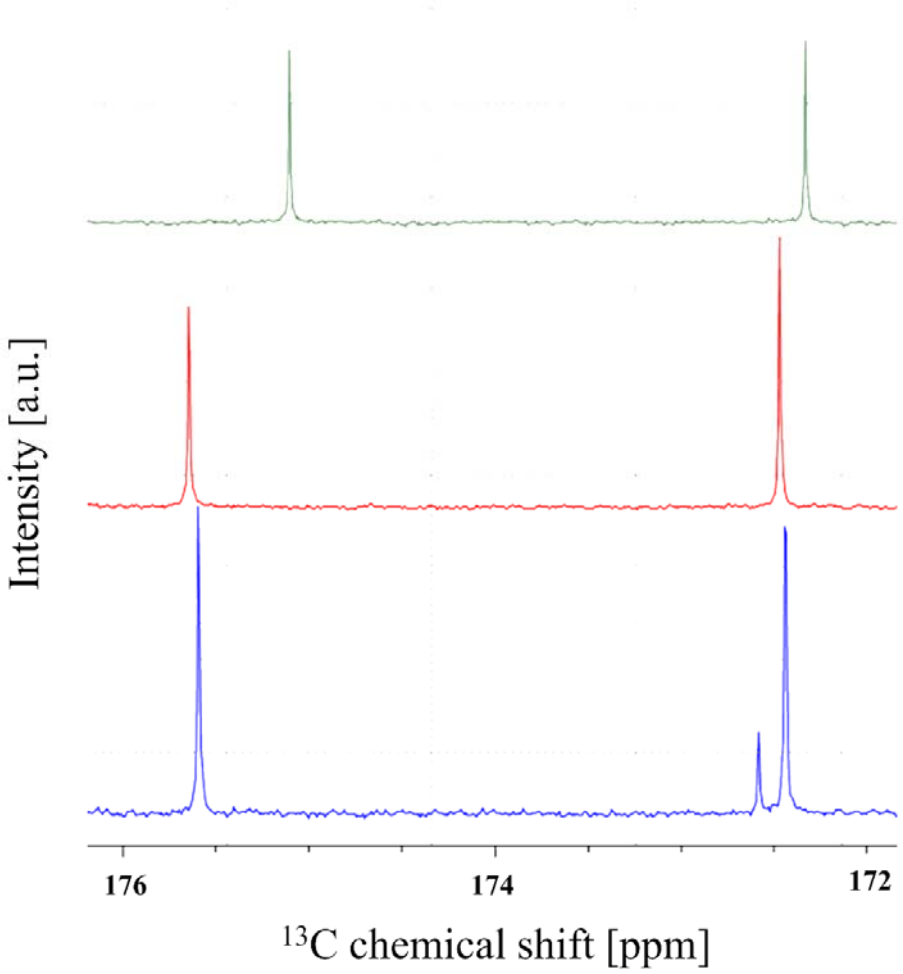

Figure 2: ^{13}C NMR spectra region between 176 and 172 ppm of MA (green), MA and EE (red) and FE, MA, EE (blue)

Consequently, the interaction was not interrupted by the addition of the model API, which showed a peak between the two carboxylic peaks of MA.

3.2.2 Amorphous form and phase behavior

An initial physical characterization of the modified matrix was based on DSC and XRPD analysis. The thermograms of the modified matrix displayed a single glass transition and no melting endotherm which supported the transparent aspect of the extrudates and hence miscibility of polymer and co-former (Figure 3).

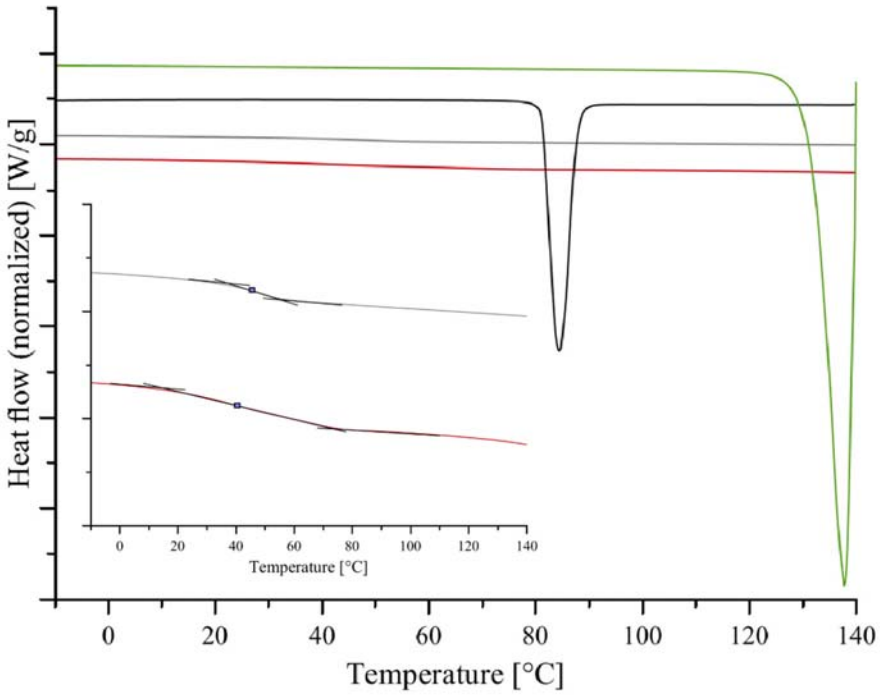

309

310 Figure 3: DSC thermograms of MA (green), FE (black), EE (grey) and MA & EE (red). Insert shows the T_g of EE and MA & EE.

311

312 These findings were in accordance with the observations provided by the XRPD experiments, where the

313 distinct peaks of crystallinity of MA were no longer visible in the modified matrix (Figure 4).

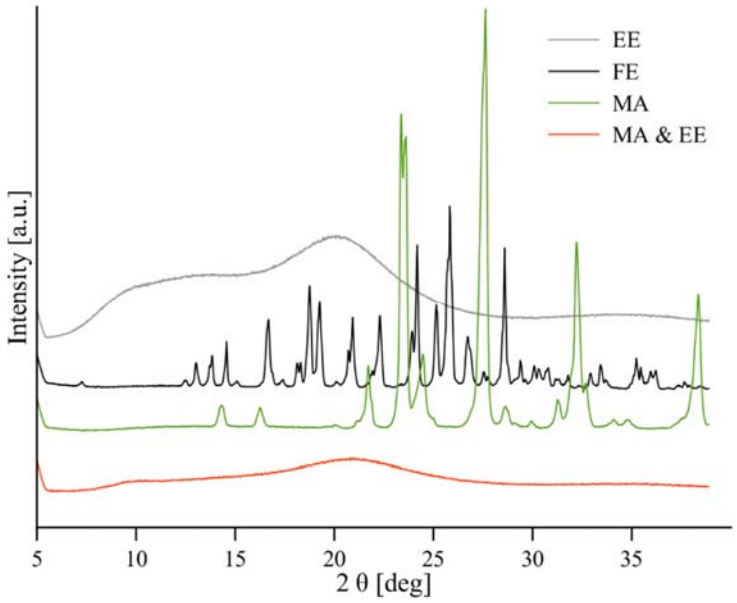

314

315 Figure 4: XRPD of MA (green), FE (black), EE (grey) and MA & EE (red)

316

The diffraction pattern and thermograms were complemented with imaging methods. The extrudates of the novel matrix exhibited a smooth surface and absence of noticeable features inside the matrix as evidenced by CLSM (data not shown). For a homogeneity analysis on a nanometer scale, extrudates were studied further by AFM phase analysis. [30] Figure 5 shows that only one phase was present in the cross section of the modified polymer matrix. Different sampling areas were scanned and no signs of separating domains that could suggest the beginning of a phase separation were observed. Imaging by AFM is a meaningful complementary analysis to other previously mentioned bulk methods. Especially phase separations of non-crystalline components are not detected by a classical XRPD analysis and it can be challenging for DSC, in which a single T_g is not always a reliable marker of homogeneity in a nanometer domain. [31] However, since the AFM imaging also suggested homogeneity across the analyzed length scales, the modified polymeric matrix was considered a glassy solution. The results therefore experimentally confirmed that a single-phase modified matrix could be obtained as hypothesized.

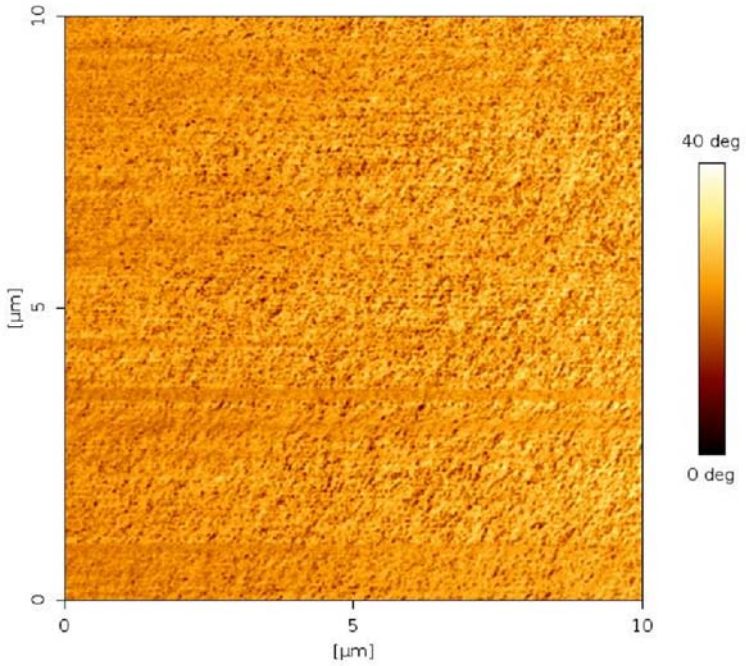

Figure 5 AFM phase images of the modified polymeric matrix (MA & EE)

3.3 Formulation of a model drug in the modified polymer matrix

An important study objective was to demonstrate the utility of the modified polymer matrix with a poorly water-soluble model drug. FE was used for this purpose and it was hypothesized that mainly the hydrophobic side chains of EE would lead to interactions with the drug, while the tertiary amine of the

polymer would mostly be interacting with MA. The assumption of hydrophobic side chain interactions was encouraged by recent studies that successfully used EE in combination with non-acidic drugs. [12,32] Based on such dispersive interactions with the lipophilic drug FE and the targeted molecular interactions with MA, Figure 6 shows an image of the assumed molecular architecture. The amine moieties of the polymer are in close proximity with carboxyl groups of the MA (shown in magenta) as it was also experimentally confirmed by the spectroscopic results of the previous section. This polymer and co-former matrix can host FE mostly between the acyl chain residues, which offers various hydrophobic interactions. The multitude of interaction options entails a favorable enthalpy of mixing with the polymer matrix, while at the same time various configurations of drug inclusion are also beneficial with respect to the entropic contribution when mixing with the drug. FE may further profit from the modified matrix because the polymeric amine is mostly masked by MA. Nitrogen-containing functional groups are known in the field of glycerides to often reduce drug solubilization of lipophilic drugs. [33] However, to verify these theoretical considerations experimentally, a proof-of-concept study was conducted. The modified matrix was first manufactured as a co-extruded material of EE and MA. The milled extrudate served as a novel polymeric matrix for HME together with FE. A comparison to this modified matrix approach was to directly compound EE, MA, and drug in a single HME step. Apart from such "direct extrusion" samples, there was also a comparison made with extruded drug with EE alone (i.e. without the co-former MA).

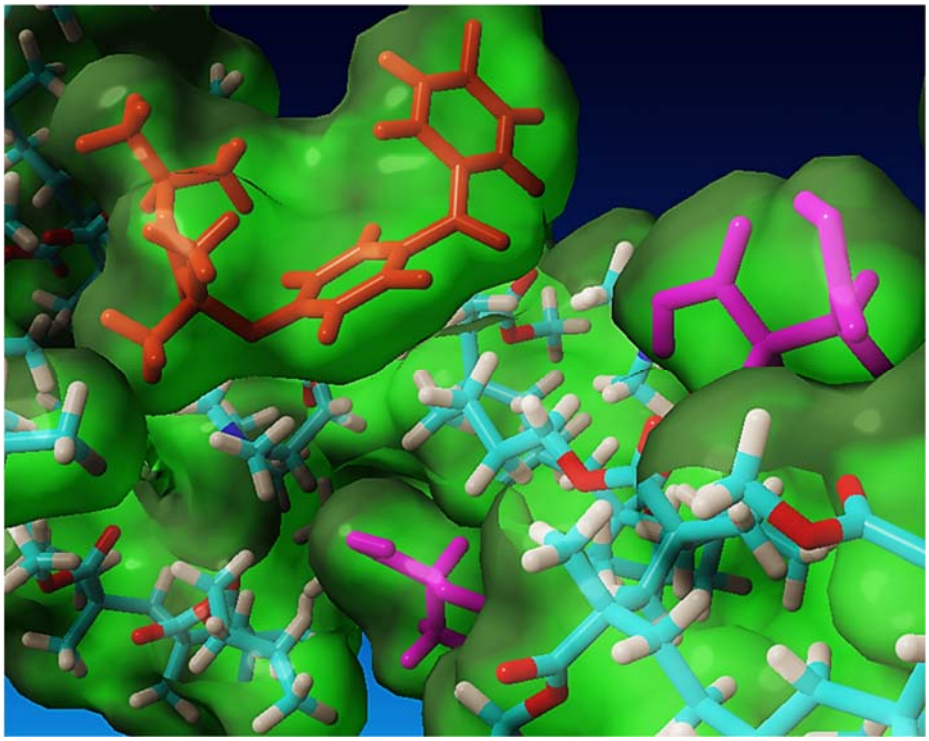

Figure 6: Visualization of the polymer matrix (EE displayed as tubes with standard color codes) together with FE (bronze tubes) and the co-former MA (magenta tubes). Only a part of the matrix is shown together with molecular surfaces for clarity of presentation. Graphic is based on YASARA version 16.12.6 using an AMBER14 force field.

3.3.1 Drug formulation processability, homogeneity and stability

A first advantage of the FE formulation with the modified matrix was observed during HME. The polymer EE was barely extruded in other studies with drugs like FE that exhibit a low melting point. [34,35] Thus, pure EE with FE produced soft strands with slow re-solidification kinetics when exiting the extrusion orifice. This processing behavior was similar to what was obtained with polymer alone and in our experience; it could be barely improved by any optimization of process parameters. Moreover, even after longer cooling a certain stickiness remained. In contrast to these results, drug formulated with the modified matrix resulted in a fast re-solidification upon extrusion and the extrudates were comparatively harder and therefore more suitable for any down-stream processing. The drug formulation with MA appeared to have similar properties to the modified matrix alone and clearly different to polymer without MA, which exhibited marked particle aggregates after milling. These qualitative observations were compared with quantitative flow properties of the milled materials in the Revolution analyzer (Table 2). [36–38] The strong cohesion forces within the bulk of EE or FE & EE formulation resulted in an increased

absolute break energy, which correlated with an increase of the avalanche angle. The comparison between pure EE and MA & EE revealed the improvement of particle flowability by the formation of the modified matrix and such improvement was also observed when drug was included as in the direct extrusion and matrix extrusion.

Table 2: Flowability and process assessment parameters for all formulations

	Absolut Break energy [mJ/kg]	Avalanche Angle [deg]	Feeding properties	Cleaning (i.e. lack of stickiness)[a]	Manufacturing
MA & EE	119.38 ± 0.27	44.33 ± 0.21	+	++	Extrusion, milling
FE & MA & EE (direct extrusion)	127.11 ± 0.12	43.67 ± 0.25	+	+	Extrusion, milling
FE & MA & EE (matrix extrusion)	124.31 ± 0.25	45.63 ± 0.12	+ +	+	Extrusion, milling, extrusion, milling
FE & EE	212.74 ± 5.14	87.4 ± 6.51	-	-	Extrusion, milling
EE powder	228.76 ± 2.19	74.80 ± 3.27	-	- -	n/a[b]

[a] For all formulations and the pure powder EE processing parameters for feeding and cleaning are evaluated qualitatively in comparison to PVP VA 64, which is known to have good flowability properties. [b] The pure EE was analyzed as received from the supplier.

The drug-containing formulation of the modified matrix as well as the reference manufactured by direct extrusion and pure drug with EE displayed no crystallinity of FE when investigated by DSC and XRPD immediately after the manufacturing. However, these classical analytical methods have limited sensitivity for small traces of initial crystallinity and moreover the beginning of an amorphous phase separation is often better detected by AFM.

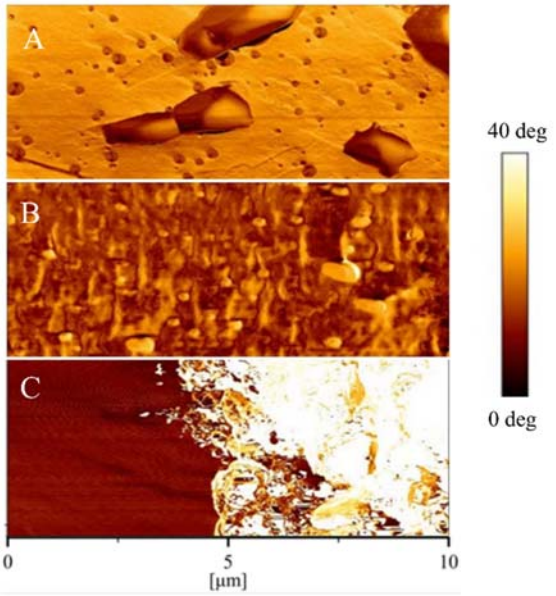

Figure 7A-C: AFM phasing images of samples from the modified polymeric systems with FE represented in the matrix extrusion (A), direct extrusion (B) in comparison to the FE & EE extrudate (C)

Figure 7 depicts AFM images of the different extrudate products with drug. Extrudates with MA displayed some micro pores (Figure 7A and 7B) but the sub-micron structure was very homogenous in case of matrix extrusion (Figure 7A) and slightly less homogenous for direct extrusion (Figure 7B) because of the formation of small domains that were only visible at a high magnification. [39] However, there was no clear indication of a phase separation in both formulations containing MA. On the other side the FE & EE extrudate (Figure 7C) showed a spreading phase separation, which is often accompanied by drug crystallization. [40]

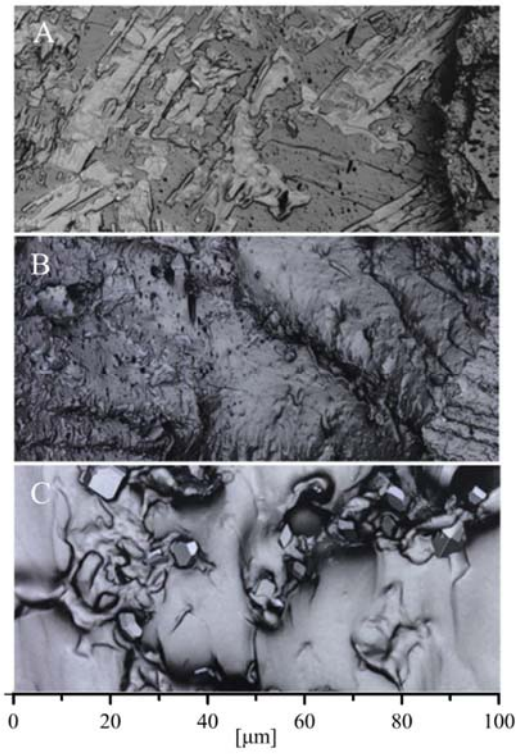

Figure 8A-C: CLSM images of the samples of drug products as modified matrix extrusion (A), direct extrusion (B) and FE & EE (C)

When a larger length scale was considered in images of CLSM, there was some crystalline material observed (Figure 8C), probably as a result of the previously described phase separation in the FE & EE formulation (Figure 7C). By contrast, in the products with MA no crystals were observed (Figure 8A and 8B), where only some surface effects were seen because of the sample preparation. In summary, the physical imaging methods performed pointed towards the observation of a phase separation (Figure 7C) and some drug crystallinity (Figure 8C) of FE & EE extrudate, which made a clear difference to the formulations with MA.

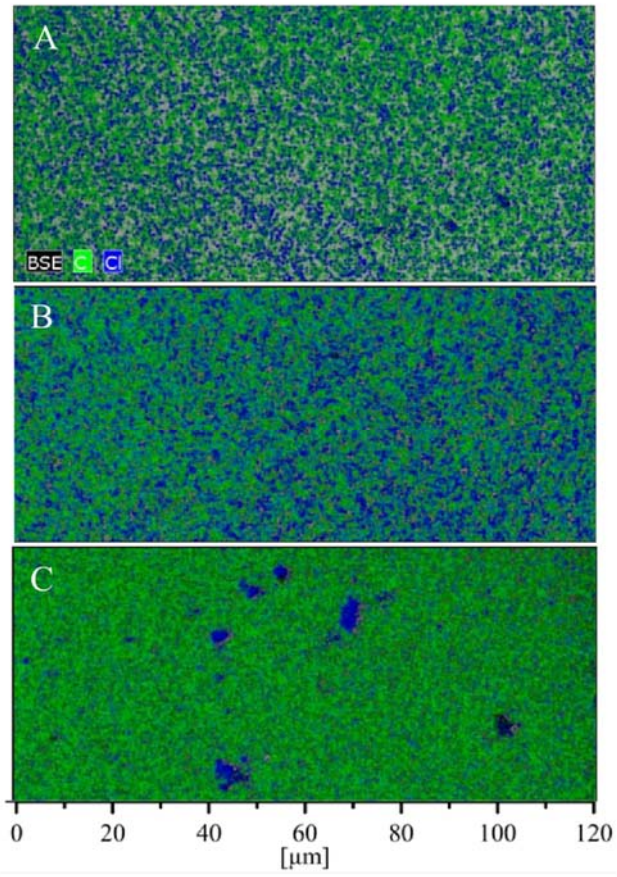

Figure 9A-C: SEM EDX images of the matrix extrusion (A), direct extrusion (B) and control (C). The green area represents the distribution of carbon, whereas the blue areas correlated with the distribution of chlorine atoms.

In addition to the physical imaging techniques, the extrudates were further investigated by the chemical imaging of SEM EDX to identify domains of FE, as detected by the distribution of chloride that is given as blue clusters in Figure 9. For the FE & EE formulation, an accumulation of mesoscopic drug clusters was evidenced. This was in agreement with findings of the inhomogeneous drug distribution in the polymer alone. As expected, there were no pronounced large drug clusters evidenced in the matrix extrusion and direct extrusion (Figure 9A and 9B). It may be that the matrix extrusion was most homogenous with respect to drug distribution but a clear differentiation to direct extrusion was hard to make by a qualitative comparison.

Finally, polarized light microscopy (PLM) was used to compare the different samples. This imaging technique is different from AFM, CLSM or SEM-EDX as a lower spatial resolution is given in this optical microscopy. However, once nuclei grow to relatively bigger crystals; PLM has the advantage that the crystals are well detected as shining birefringent structures (data not shown). This was only detected in samples of FE with EE after two weeks storage at room temperature, whereas the samples of melt extrusion and direct extrusion did not show any crystals in line with the aforementioned results from AFM, CLSM and SEM-EDX.

3.3.2 Amorphous dissolution benefits

Dissolution of the formulations was conducted, using the method described for quality control, [20] to identify any potential difference in the formulations with respect to their dissolution behavior. The scope was to reveal potential differences, which should be differentiated from the rationale to mimic *in vivo* conditions, since this would otherwise require biorelevant dissolution testing. [20,41,42]

For a comparison, all samples were milled in a vibration mill for one minute. Although, all samples were treated equally, the FE & EE formulation showed very poor milling processability, which resulted in agglomeration under different milling conditions. This was likely a consequence of the earlier described technical issues of FE & EE with especially the pronounced cohesion of the material. Probably as a result of this difference, the comparison between the two extruded formulations and the physical mixture showed a clear improvement in drug release for the extruded formulations. Since the FE & EE formulation did not result in a comparable processed formulation, which was also visible in the dissolution behavior, it can be concluded that the direct extrusion and the matrix extrusion were a clear advancement in terms of drug release compared to the physical mixture (Figure 10). In accordance with the previous analytical results, which showed phase separation and recrystallization of FE & EE, repeated dissolution experiments over time may further reveal differences in dissolution performance during storage.

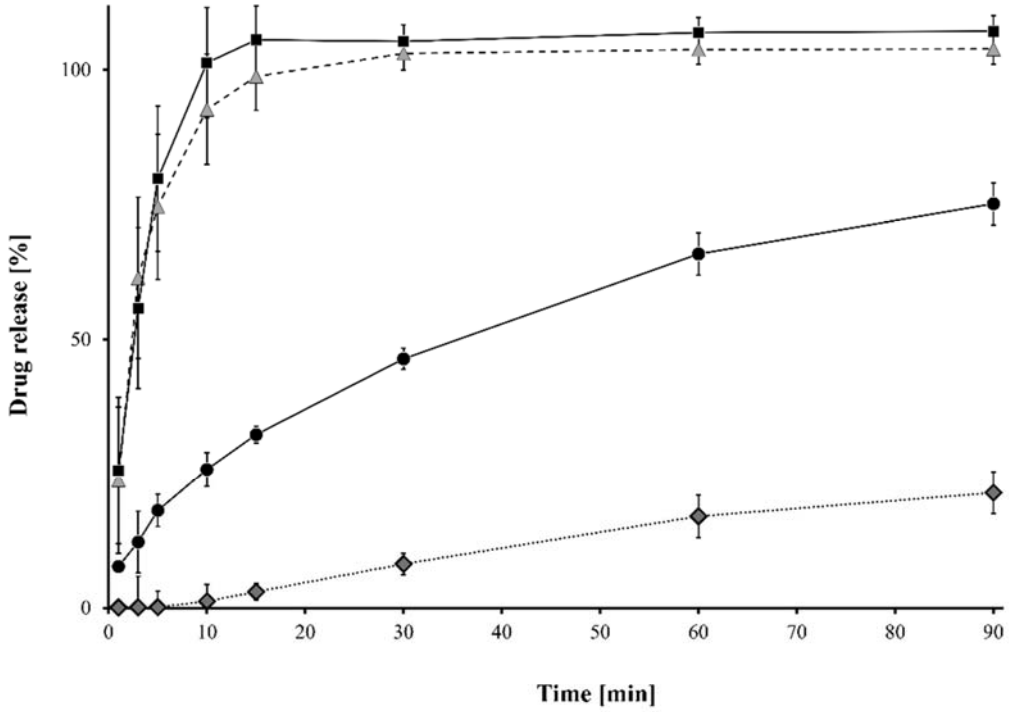

Figure 10: Dissolution curves of the matrix extrusion (black squares), direct extrusion (grey triangles), FE & EE extrudate (black dots) and physical mixture FE & EE & MA (grey diamonds)

4 Conclusions

Various aspects in HME processing of amorphous solid dispersions limit the selection of pharmaceutical polymers for a given drug. This work started from a molecular rationale to modify a polymer matrix of EE physically by co-extruding it with a bi-valent acid. The molecular rationale differs greatly from classic formulation approaches, where plasticizer or anti-plasticizer are screened empirically without a clear molecular rationale. Therefore, the described approach offers new opportunities based on molecular pharmaceutics to modify a polymeric matrix by means of selected small molecular additives. Such a theoretically designed modified matrix was experimentally verified as a glassy solution that was homogenous at the different length scales studied. Moreover, spectroscopic methods confirmed the assumed molecular interactions. An explicit objective was to show benefits of the new polymeric matrix with a model drug FE. This drug was selected to interact primarily with the acyl-side chains of the

polymer via hydrophobic interactions, while the masked tertiary amine of EE would primarily interact with the co-former MA. Benefits of the modified matrix compared to amorphous dispersions of FE in EE without co-former where demonstrated for technical feasibility but also with respect to drug distribution and lack of crystalline material. Moreover, drug dissolution was enhanced for the direct extrusion and matrix extrusion formulations, when compared to the reference formulations of pure drug and polymer.

Interesting findings were the slight differences in technical feasibility as well as drug distribution between direct extrusion and matrix extrusion with the additive MA. This could be used potentially by excipient suppliers, which would be able to offer directly a modified matrix to the pharmaceutical industry to widen the selection of suitable polymeric vehicles for HME. This approach to modify the polymeric matrix based on a molecular rationale is highly interesting and more research could target specific solubility parameters that are currently not available with existing pharmaceutical polymers for HME. The idea to modify polymers non-chemically can be harnessed in the future to target a specific increase or decrease of the glass transition, or for example, to tailor polymer swelling in water for a desired drug release. Finally, research in the future could emphasize the effects of modified matrices on long-term physical stability of amorphous solid dispersions.

Declarations

Conflict of interest

The authors declare that they have no conflicts of interest to disclose.

Funding

This project has received funding from the European Union's Horizon 2020 Research and Innovation Program under grant agreement No 674909.

Acknowledgement

Special thanks to Theodor Bühler for his assistance in the analysis of FTIR and SEM data.

Literature

(1) Serajuddin, A. T. M. Solid Dispersion of Poorly Water-soluble Drugs: Early Promises, Subsequent Problems, and Recent Breakthroughs. *J. Pharm. Sci.* **1999**, *88* (10), 1058–1066.

(2) Hancock, B. C.; Parks, M. What Is the True Solubility Advantage for Amorphous Pharmaceuticals? *Pharm. Res.* **2000**, *17* (4), 397–404.

(3) Hancock, B. C.; Zografi, G. Characteristics and Significance of the Amorphous State in Pharmaceutical Systems. *J. Pharm. Sci.* **1997**, *86* (1), 1–12.

(4) Janssens, S.; Van den Mooter, G. Review: Physical Chemistry of Solid Dispersions. *J. Pharm. Pharmacol.* **2009**, *61* (12), 1571–1586.

(5) Wyttenbach, N.; Kuentz, M. Glass-Forming Ability of Compounds in Marketed Amorphous Drug Products. *Eur. J. Pharm. Biopharm.* **2017**, *112*, 204–208.

(6) Elder, D. P.; Kuentz, M.; Holm, R. Pharmaceutical Excipients — Quality, Regulatory and Biopharmaceutical Considerations. *Eur. J. Pharm. Sci.* **2016**, *87*, 88–99.

(7) Desai, D.; Sandhu, H.; Shah, N.; Malick, W.; Zia, H.; Phuapradit, W.; Vaka, S. R. K. Selection of Solid-State Plasticizers as Processing Aids for Hot-Melt Extrusion. *J. Pharm. Sci.* **2018**, *107* (1), 372–379.

(8) Newman, A.; Reutzel-Edens, S. M.; Zografi, G. Coamorphous Active Pharmaceutical Ingredient–Small Molecule Mixtures: Considerations in the Choice of Coformers for Enhancing Dissolution and Oral Bioavailability. *J. Pharm. Sci.* **2018**, *107* (1), 5–17.

(9) Chavan, R. B.; Thipparaboina, R.; Kumar, D.; Shastri, N. R. Co Amorphous Systems: A Product Development Perspective. *Int. J. Pharm.* **2016**, *515* (1–2), 403–415.

(10) Laitinen, R.; Löbmann, K.; Grohganz, H.; Priemel, P.; Strachan, C. J.; Rades, T. Supersaturating Drug Delivery Systems: The Potential of Co-Amorphous Drug Formulations. *Int. J. Pharm.* **2017**, *532* (1), 1–12.

(11) Higashi, K.; Seo, A.; Egami, K.; Otsuka, N.; Limwikrant, W.; Yamamoto, K.; Moribe, K.

Mechanistic Insight into the Dramatic Improvement of Probucol Dissolution in Neutral Solutions by Solid Dispersion in Eudragit E PO with Saccharin. *J. Pharm. Pharmacol.* **2016**, *68* (5), 655–664.

(12) Saal, W.; Ross, A.; Wyttenbach, N.; Alsenz, J.; Kuentz, M. Unexpected Solubility Enhancement of Drug Bases in the Presence of a Dimethylaminoethyl Methacrylate Copolymer. *Mol. Pharm.* **2018**, *15* (1), 186–192.

(13) Saal, W.; Ross, A.; Wyttenbach, N.; Alsenz, J.; Kuentz, M. A Systematic Study of Molecular Interactions of Anionic Drugs with a Dimethylaminoethyl Methacrylate Copolymer Regarding Solubility Enhancement. *Mol. Pharm.* **2017**, *14* (4), 1243–1250.

(14) Wu, W.; Löbmann, K.; Rades, T.; Grohganz, H. On the Role of Salt Formation and Structural Similarity of Co-Formers in Co-Amorphous Drug Delivery Systems. *Int. J. Pharm.* **2018**, *535* (1–2), 86–94.

(15) Dengale, S. J.; Grohganz, H.; Rades, T.; Löbmann, K. Recent Advances in Co-Amorphous Drug Formulations. *Adv. Drug Deliv. Rev.* **2016**, *100*, 116–125.

(16) Laitinen, R.; Löbmann, K.; Grohganz, H.; Strachan, C.; Rades, T. Amino Acids as Co-Amorphous Excipients for Simvastatin and Glibenclamide: Physical Properties and Stability. *Mol. Pharm.* **2014**, *11* (7), 2381–2389.

(17) Bookwala, M.; Thipsay, P.; Ross, S.; Zhang, F.; Bandari, S.; Repka, M. A. Preparation of a Crystalline Salt of Indomethacin and Tromethamine by Hot Melt Extrusion Technology. *Eur. J. Pharm. Biopharm.* **2018**, *131*, 109–119.

(18) *Revolution Powder Analyzer User Manual*; Mercury Scientific Inc.: Newtown.

(19) Tay, J. Y. S.; Liew, C. V.; Heng, P. W. S. Powder Flow Testing: Judicious Choice of Test Methods. *AAPS PharmSciTech* **2017**, *18* (5), 1843–1854.

(20) Grady, H.; Elder, D.; Webster, G. K.; Mao, Y.; Lin, Y.; Flanagan, T.; Mann, J.; Blanchard, A.; Cohen, M. J.; Lin, J.; et al. Industry's View on Using Quality Control, Biorelevant, and Clinically Relevant Dissolution Tests for Pharmaceutical Development, Registration, and Commercialization. *J. Pharm. Sci.* **2018**, *107* (1), 34–41.

(21) Meng, F.; Dave, V.; Chauhan, H. Qualitative and Quantitative Methods to Determine Miscibility

in Amorphous Drug–polymer Systems. *Eur. J. Pharm. Sci.* **2015**, *77*, 106–111.

(22) Van Eerdenbrugh, B.; Taylor, L. S. An Ab Initio Polymer Selection Methodology to Prevent Crystallization in Amorphous Solid Dispersions by Application of Crystal Engineering Principles. *CrystEngComm* **2011**, *13* (20), 6171.

(23) Wyttenbach, N.; Janas, C.; Siam, M.; Lauer, M. E.; Jacob, L.; Scheubel, E.; Page, S. Miniaturized Screening of Polymers for Amorphous Drug Stabilization (SPADS): Rapid Assessment of Solid Dispersion Systems. *Eur. J. Pharm. Biopharm.* **2013**, *84* (3), 583–598.

(24) Kojima, T.; Higashi, K.; Suzuki, T.; Tomono, K.; Moribe, K.; Yamamoto, K. Stabilization of a Supersaturated Solution of Mefenamic Acid from a Solid Dispersion with EUDRAGIT® EPO. *Pharm. Res.* **2012**, *29* (10), 2777–2791.

(25) Singh, S.; Parikh, T.; Sandhu, H. K.; Shah, N. H.; Malick, A. W.; Singhal, D.; Serajuddin, A. T. M. Supersolubilization and Amorphization of a Model Basic Drug, Haloperidol, by Interaction with Weak Acids. *Pharm. Res.* **2013**, *30* (6), 1561–1573.

(26) Parikh, T.; Serajuddin, A. T. M. Development of Fast-Dissolving Amorphous Solid Dispersion of Itraconazole by Melt Extrusion of Its Mixture with Weak Organic Carboxylic Acid and Polymer. *Pharm. Res.* **2018**, *35* (7), 127.

(27) Alhalaweh, A.; Alzghoul, A.; Mahlin, D.; Bergström, C. A. S. Physical Stability of Drugs after Storage above and below the Glass Transition Temperature: Relationship to Glass-Forming Ability. *Int. J. Pharm.* **2015**, *495* (1), 312–317.

(28) Baranska, H.; Kuduk-Jaworska, J.; Szostak, R.; Romaniewska, A. Vibrational Spectra of Racemic and Enantiomeric Malic Acids. *J. Raman Spectrosc.* **2003**, *34* (1), 68–76.

(29) Kasten, G.; Nouri, K.; Grohganz, H.; Rades, T.; Löbmann, K. Performance Comparison between Crystalline and Co-Amorphous Salts of Indomethacin-Lysine. *Int. J. Pharm.* **2017**, *533* (1), 138–144.

(30) Lauer, M. E.; Siam, M.; Tardio, J.; Page, S.; Kindt, J. H.; Grassmann, O. Rapid Assessment of Homogeneity and Stability of Amorphous Solid Dispersions by Atomic Force Microscopy—From Bench to Batch. *Pharm. Res.* **2013**, *30* (8), 2010–2022.

(31) Qian, F.; Huang, J.; Zhu, Q.; Haddadin, R.; Gawel, J.; Garmise, R.; Hussain, M. Is a Distinctive

Single Tg a Reliable Indicator for the Homogeneity of Amorphous Solid Dispersion? *Int. J. Pharm.* **2010**, *395* (1–2), 232–235.

(32) Saal, W.; Wyttenbach, N.; Alsenz, J.; Kuentz, M. Interactions of Dimethylaminoethyl Methacrylate Copolymer with Non-Acidic Drugs Demonstrated High Solubilization in Vitro and Pronounced Sustained Release in Vivo. *Eur. J. Pharm. Biopharm.* **2018**, *125*, 68–75.

(33) Persson, L. C.; Porter, C. J. H.; Charman, W. N.; Bergström, C. A. S. Computational Prediction of Drug Solubility in Lipid Based Formulation Excipients. *Pharm. Res.* **2013**, *30* (12), 3225–3237.

(34) Li, S.; Tian, Y.; Jones, D. S.; Andrews, G. P. Optimising Drug Solubilisation in Amorphous Polymer Dispersions: Rational Selection of Hot-Melt Extrusion Processing Parameters. *AAPS PharmSciTech* **2016**, *17* (1), 200–213.

(35) Qi, S.; Gryczke, A.; Belton, P.; Craig, D. Q. M. Characterisation of Solid Dispersions of Paracetamol and EUDRAGIT® E Prepared by Hot-Melt Extrusion Using Thermal, Microthermal and Spectroscopic Analysis. *Int. J. Pharm.* **2008**, *354* (1–2), 158–167.

(36) Hurychová, H.; Kuentz, M.; Šklubalová, Z. Fractal Aspects of Static and Dynamic Flow Properties of Pharmaceutical Excipients. *J. Pharm. Innov.* **2018**, *13* (1), 15–26.

(37) Hancock, B. C.; Vukovinsky, K. E.; Brolley, B.; Grimsey, I.; Hedden, D.; Olsofsky, A.; Doherty, R. A. Development of a Robust Procedure for Assessing Powder Flow Using a Commercial Avalanche Testing Instrument. *J. Pharm. Biomed. Anal.* **2004**, *35* (5), 979–990.

(38) Nalluri, V. R.; Puchkov, M.; Kuentz, M. Toward Better Understanding of Powder Avalanching and Shear Cell Parameters of Drug–excipient Blends to Design Minimal Weight Variability into Pharmaceutical Capsules. *Int. J. Pharm.* **2013**, *442* (1–2), 49–56.

(39) Adler, C.; Schönenberger, M.; Teleki, A.; Kuentz, M. Molecularly Designed Lipid Microdomains for Solid Dispersions Using a Polymer/Inorganic Carrier Matrix Produced by Hot-Melt Extrusion. *Int. J. Pharm.* **2016**, *499* (1–2), 90–100.

(40) Schram, C. J.; Beaudoin, S. P.; Taylor, L. S. Impact of Polymer Conformation on the Crystal Growth Inhibition of a Poorly Water-Soluble Drug in Aqueous Solution. *Langmuir* **2015**, *31* (1), 171–179.

(41) Galia, E.; Nicolaides, E.; Hörter, D.; Löbenberg, R.; Reppas, C.; Dressman, J. B. Evaluation of

Various Dissolution Media for Predicting in Vivo Performance of Class I and II Drugs. *Pharm. Res.* **1998**, *15* (5), 698–705.

(42) Vertzoni, M.; Fotaki, N.; Nicolaides, E.; Reppas, C.; Kostewicz, E.; Stippler, E.; Leuner, C.; Dressman, J. Dissolution Media Simulating the Intralumenal Composition of the Small Intestine: Physiological Issues and Practical Aspects. *J. Pharm. Pharmacol.* **2004**, *56* (4), 453–462.